Smart pyrometry for combined sample temperature and reflectance measurements in molecular-beam epitaxy

K. A. Bertness
National Institute of Standards and Technology, Optoelectronics Division, Boulder, Colorado 80303

(Received 10 October 1999; accepted 7 February 2000)

Improved accuracy of measurements of semiconductor wafer temperature is demonstrated in a normal-incidence optical reflectance spectroscopy system that has been modified to allow rapid switching between the measurement of wafer reflectance and wafer emission. The resulting optical system is capable of "smart" pyrometry, in which the emissivity is determined each time the temperature is measured. Measurements during heteroepitaxial growth show that the data from smart pyrometry typically differ from those of conventional pyrometry by 5–10 °C, and occasionally by as much as 20 °C for multilayer structures of AlGaAs and GaAs. Theory, experimental procedures, and calibration procedures are discussed. [S0734-211X(00)05903-5]

I. INTRODUCTION

In this article, a method is described for improving the measurements of sample temperature in molecular-beam epitaxy (MBE) systems. The equipment consists of a multifunctional optical system that can rapidly switch between measuring wafer reflectance and wafer emission. As in most MBE systems, wafer temperature is measured pyrometrically, that is, by measuring the intensity of the emitted light over a narrow range of wavelengths in the infrared region of the spectrum. This emitted thermal radiation is often referred to as "blackbody radiation," although the primary difficulty in accurately interpreting the data is the fact that the sample is *not* a true blackbody. A semiconductor wafer during epitaxial growth has an emissivity that varies significantly both in time and with wavelength. In the multifunctional optical system, the emissivity is determined as needed from a separate measurement of reflectance at the wavelength of interest.

Measurement of wafer temperature in MBE has a long history. Stationary thermocouples and uncorrected optical pyrometers remain the most widely used techniques for sensing wafer temperature, though the shortcomings of these techniques are well known. Accuracy can be significantly improved by using emissivity-corrected pyrometry,[1–3] the technique described here, or band-edge thermometry,[4,5] in which the band-gap energy of the substrate is measured and converted to a temperature using a calibration curve that depends on the epilayer material, substrate material, doping and polish. Systems based on both techniques are available commercially though they are not widely used, partly because of the cost and the inconvenience of integrating the thermometry systems with the existing MBE growth systems. The measurement system described in this article differs from previous work in the optical components, signal electronics, and calibration techniques used.

The basic principles of pyrometry needed to interpret the data will be reviewed briefly in the theory section. The experiment section includes a detailed description of the equipment and discussion of sample wobble effects. Next, a few examples of experimental data will be shown and discussed to illustrate the utility and limitations of the technique. These examples include the use of an Al–Si eutectic sample to calibrate the optical collection efficiency of the system. The system has shown itself to be suitable for measuring sample temperatures of 400 °C and above, although interference from light emitted by hot effusion cells and scattered off the sample into the pyrometry collection system is a significant effect, particularly at wafer temperatures below 550 °C.

II. THEORY

The temperature measurement makes use of the principle of detailed balance, which states that for specular, opaque specimens, the sum of the emissivity $\epsilon(\lambda)$ and reflectance $R(\lambda)$ *at each wavelength* is equal to one.[6] The specimen's emissivity is therefore determined by measuring its reflectance at the same wavelength used to measure its temperature. This emissivity varies with both wavelength and time and therefore cannot be eliminated from the equations merely by using emission data taken at two different wavelengths (two-color pyrometry). Thermodynamic balance of photon populations also states that the photons emitted at any one wavelength in any one direction follow a Planck distribution. For analyzing our data, we write the pyrometry signal S as measured at the detector as

$$S=\eta(\lambda)\varepsilon(\lambda)f(T,\lambda)\,d\Omega, \quad (1)$$

where $\eta(\lambda)$ represents the efficiency of the collecting optics, detector, and electronic amplification of the signal, $f(T,\lambda)$ is the Planck distribution, and $d\Omega$ is the effective solid angle of the light collected from the sample. The Planck distribution depends on wavelength λ, temperature T, Planck's constant h, the speed of light c, and the Boltzmann constant k as $2hc^2(\delta\lambda/\lambda^5)\{1/\exp(hc/\lambda kT)-1]\}$. We can make the short-wavelength approximation that 1 is negligible compared to $\exp(hc/\lambda kT)$, group the constants $2hc^2(\delta\lambda/\lambda^5)\eta(\lambda)d\Omega$ together into a factor S_0, define the experimentally measured quantity $S^*=S/(1-R)$, and solve for temperature

$$T=(hc/\lambda k)/\ln(S_0/S^*). \quad (2)$$

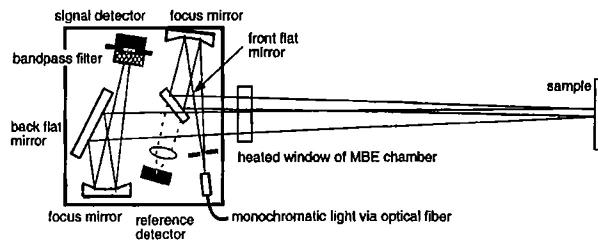

FIG. 1. Schematic of smart pyrometer and optical reflectance system. The front flat mirror is rotated in and out of the sample line of sight to switch between measuring sample reflectance (and hence emissivity) and the sample "blackbody" emission intensity. The optical components are mounted on a 20 cm × 20 cm optical breadboard that is bolted to the normal-incidence port of the MBE chamber.

Using the center wavelength of the filter of 925.0 nm, the factor in the numerator is 15 550 K. Calibration of the system therefore consists of determining the value of S_0 appropriate for the wavelength, optics, and signal amplification. Because the signal varies by more than a factor of 10 over the range of typical MBE growth temperatures, the software that implements the equation also takes into account the different gain factors used by the detector amplifier. Implicit in this process is a calibration of the reflectance measurements so that absolute reflectance can be determined.

III. EXPERIMENT

The overall layout of the optical system is illustrated in Fig. 1. The mounts used for the flat mirrors allow them to be flipped in and out of line of sight with the substrate without losing beam alignment. The rotating action of the front mirror is computer controlled to allow rapid switching between measurements of wafer emission and reflectance. The mirrors and detectors are arranged on a 20 cm × 20 cm optical breadboard that is clamped to a heated quartz window[7] located about 65 cm from the substrate at normal incidence. The intensity of the emission from the wafer is measured over a wavelength range of 10 nm by placing a bandpass filter centered at 925 nm in front of the detector with the front flat mirror rotated down. The bandpass filter can be rotated out of the beam path in order to acquire a broadband reflectance spectrum, a feature that increases the versatility of the instrument but which is not necessary for temperature measurement. GaAs and InP substrates are opaque at 925 nm for the minimum signal temperature of 400 °C, but other substrates may lead to false readings because thermal radiation from the heater plate is partially transmitted. In earlier versions of the system, the bandpass filter was centered at 1000 nm, and substrate transparency effects were observed.[8] The amplified emission signal at 925 nm is similar in magnitude to the signal at 1000 nm for the same wafer temperature because the optical collection efficiency is higher at 925 nm.

For reflectance measurements, the front flat mirror is rotated up into a beam of monochromatic light tuned to the center wavelength of the detector filter. This light is delivered by a large-core optical fiber from a monochromator (bandpass of 1.5 nm at 925 nm) attached to a 75 W xenon arc lamp (not shown). An iris removes light emitted from the higher order modes of the fiber before the beam reaches the focusing mirror. The beam diameter is about 15 mm at the front focus mirror, 4 mm at the wafer surface, 10 mm where it exits the vacuum window, and 1.5 mm at the signal detector. The collecting optics are arranged so that an image of the wafer is formed at the plane of the signal detector. This arrangement minimizes collection of stray light in pyrometric mode and reduces sensitivity to beam wobble in reflection mode. The front mirror pair is placed so that when the flat mirror is rotated out of the incoming light beam, the beam is focused onto a second silicon reference detector. This signal is used periodically to normalize the absolute reflectance calibration for changes in lamp intensity and lamp-monochromator-fiber coupling.

The light beam is chopped at approximately 160 Hz and the signal processed through a lock-in amplifier to distinguish between the reflectance signal and background light or wafer emission. The detectors are silicon photodiodes 5 mm in diameter connected to preamplifiers with computer-controlled gain. Typical reflectance signal currents are on the order of 10 nA, and the pyrometric signal for a wafer temperature of 600 °C is about 1 nA. The data acquisition system monitors four analog signals, namely, the reflectance signal as processed by the lock-in amplifier, the reference photodiode signal, the direct signal from the reflectance detector (used for measuring wafer emission), and a trigger signal proportional to the angular position of the substrate manipulator as it rotates. A significant body of software has been developed to automate the data acquisition and interpretation.

The changes in reflectance signal intensity from the slight wobbling motion of the wafer as it rotates are compensated by checking substrate alignment for each new substrate while hot and acquiring a normalization curve for the signal as a function of rotation angle.[9] The manufacturer of the substrate manipulator tightened tolerances in the rotation mechanism and thereby reduced the intrinsic wobble to less than ±0.2° for rigid substrate holder rings. Substrates mounted with thin metal insert plates can show up to 0.5° additional wobble depending on how the metal fingers holding the wafers are positioned. For most substrates, the rotation normalization factor is between 0.95 and 1.0. The degree to which the factor differs from 1.0 is probably due to variable transmittance of the vacuum chamber window where the return beam sweeps through a rough circle whose diameter increases with wobble angle. For larger wobble angles, the beam is partly blocked by the window edge and/or the front mirror mount during sections of the rotation. Therefore, absolute reflectance values are normalized to the maximum signal measured during the rotation cycle. The pyrometric signal also often shows rotation-related variations. These effects can be minimized by realigning the reflectance beam for each new sample so that the bandpass filter is at normal incidence to the center of rotation of the incoming beam.

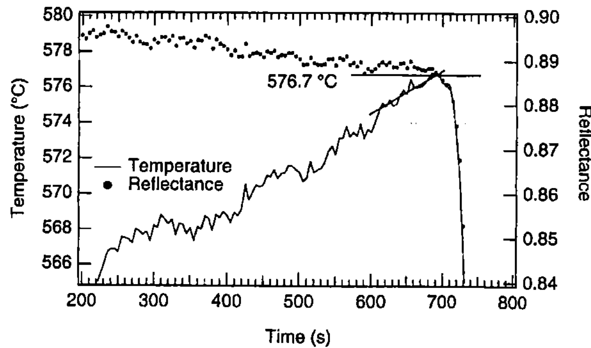

FIG. 2. Wafer temperature and reflectance as a function of time during slow heating of an Al–Si eutectic specimen. The reflectance of the wafer at room temperature was 0.91 at room temperature. At the eutectic transition, the surface roughened, and the reflectance as well as the apparent temperature dropped dramatically. These results show that the calibration constant $\ln(S_0)$, related primarily to the solid angle collected by the emission signal optics, is properly selected.

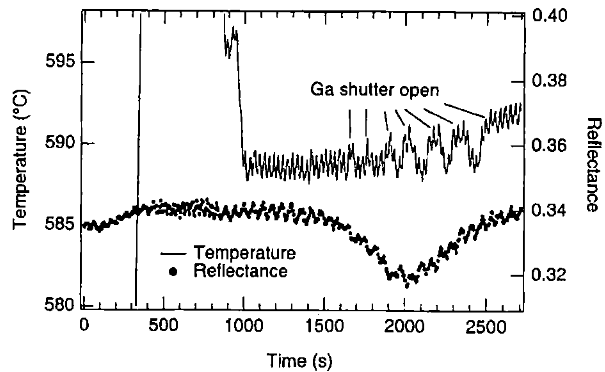

FIG. 3. Wafer temperature and reflectance as a function of time during oxide desorption and initial buffer layer growth on a GaAs substrate. The data illustrate the typical variations observed in measurement of wafer temperature (±0.5 °C) as the sample rotates, and the slight heating of the wafer by thermal radiation emitted from the Ga evaporation cell.

The absolute reflectance measurements are calibrated using a Si wafer that has been coated with Al and then MgF_2 to provide a stable, broadband reflective surface. The mirror wafer is measured *ex situ* against a reflectivity standard in a spectrophotometer and then transferred into the growth system. The ratio of the reflectance signal to the reference-detector signal is measured over the wavelength range of interest, and a correction factor is calculated from the measured values and the known reflectance of the mirror. This factor can be updated each time the reference signal is measured. The uncertainty in the reflectance measurements made following these calibrations is about 1%, with roughly equal contributions from the uncertainty in the reflectivity standard used in the spectrophotometer and the noise in the reference detector signal.

The simplest way to get an approximate calibration of the smart pyrometer is to adjust the S_0 parameter to achieve agreement with a conventional pyrometer when measuring the temperature of bare GaAs wafers. The conventional pyrometer should be set to use the emissivity measured with the calibrated optical reflectance system. Bare GaAs wafers typically have reflectance in the range from 0.33 to 0.35, and comparison with a standard pyrometer led to the selection of $\ln(S_0)=18.55$ as the appropriate value for our system. The accuracy of this number can be improved by monitoring the temperature of an Al/Si eutectic specimen while slowly heating the specimen through the eutectic transition at 577 °C. The data given in Fig. 2 show the clear and sudden decline in sample reflectance as the eutectic formation roughens the surface. The Al/Si wafer was prepared by evaporating about 100 nm of Al onto a clean silicon wafer. The reflectance of the wafer was measured *ex situ*, and in order to avoid excessive oxidation of the Al layer, the wafer was loaded into the vacuum chamber within a few hours of the Al evaporation. The reflectance calibration was adjusted to match the *ex situ* measurement, and the final approach to the eutectic transition was made at a rate of 0.033 °C/s. The eutectic specimen, being opaque in the infrared, is actually hotter than the substrate manipulator thermocouple, in contrast to a typical GaAs wafer that runs about 100–150 °C cooler than the thermocouple. The data show that the temperature can be determined with an uncertainty of 0.5 °C, and that no further adjustment of the $\ln(S_0)$ parameter was needed.

IV. RESULTS

Figure 3 illustrates some of the capabilities of the instrument by following the reflectance and the temperature of a GaAs wafer during initial heating to remove native oxides and early buffer layer growth. The substrate was rotating under arsenic flux during the entire period shown. The pyrometry signal first became distinguishable from detector noise at about 380 °C (not shown). The substrate was heated above 640 °C to ensure complete oxide removal, then cooled for buffer layer growth. The reflectance signal became noisier after heating due to a slight shift in the wobble of the substrate. The temperature measurement oscillated by about ±1 °C due to the variable optical collection efficiency as the sample rotated. The actual wafer temperature also increased by 2–3 °C due to radiative heating from the Ga evaporation cell when the shutter is open.[10] Data taken with finer time resolution confirmed that the time scale of this temperature change is consistent with heating rather than scattering of stray light, the latter of which would instantaneously change the apparent wafer temperature. This figure also shows an interesting consequence of buffer layer growth: the surface roughened at first as shown by the slight decrease in substrate reflectivity. Reflection high-energy electron diffraction (RHEED) patterns were spotty rather than streaky during this period. As the growth/growth interruption cycles proceeded, the reflectance and the RHEED pattern improved until the initial substrate reflectivity was recovered and the RHEED pattern consisted of clear 2×4 reconstruction streaks.

An example of data taken during an epitaxial growth run is given in Fig. 4. The specimen structure is a Bragg-reflector stack designed for a high-reflectance band centered at 980 nm at room temperature. The structure consists of alternating

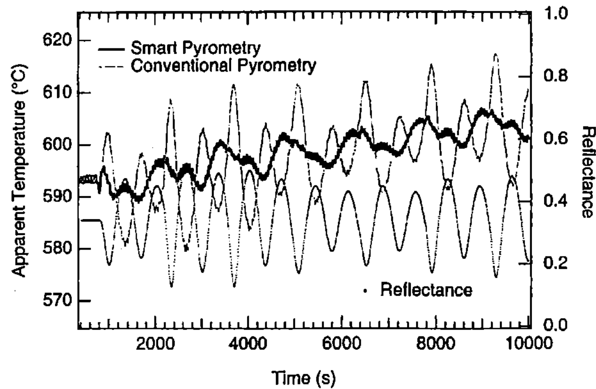

FIG. 4. Comparison of sample temperatures derived from smart pyrometry (solid line) and conventional pyrometry (light gray line) as a function of time during growth of a Bragg reflector stack. Reflectance data (dots) is plotted for the same period against the right axis.

81–83 nm AlGaAs layers with Al mole fraction greater than 0.90 and 208 nm layers of GaAs, with growth times of 213–250 and 1160 s, respectively. The graph also includes the conventional pyrometric temperature corresponding to the same emission signal interpreted with an assumption of constant emissivity (0.76). The optical reflectance system was programmed to acquire a reflectance value every 5 s and a temperature value every 20 s. The substrate heater power was varied to maintain constant temperature at the substrate manipulator thermocouple throughout the time period shown. The wafer temperature initially went through some small shifts down then up from cooling during a growth interruption around 780 s followed by radiative heating when the Al shutter opened.

As the growth progressed, the apparent temperature as determined by conventional pyrometry (light gray line) varied dramatically due to the large changes in wafer emissivity. This effect has been used to characterize the thickness and composition of epitaxial layers because in essence it tracks the interference fringes in the wafer reflectance.[2,11–13] The conventional pyrometer readings are not only inaccurate in magnitude, they also indicate temperatures changes of the wrong sign. When the wafer is cooling due to increased emissivity, the conventional pyrometer falsely indicates that the wafer is heating up. The emissivity-corrected temperature readings (black line) show that there is a real shift in the wafer temperature as its broadband radiative cooling-losses change. The changes agree with results from other temperature techniques and wafer heat transfer calculations.[4] The temperature drift can be significant; there is a variation of 15 °C between the minimum and maximum wafer temperatures measured in this time frame. We have seen that even the growth of relatively simple structures, such as the lower half of a laser diode, will cause a temperature drift of about 7 °C. The next step in instrumentation development is to use the measured temperature to correct the setpoint of the substrate heater through a nested control algorithm.[4]

The primary limitation on the accuracy of the pyrometer is the false increase in apparent temperature caused by light scattered into the collection optics from effusion cells. The effect is largest for small samples surrounded by rough wafer holder plates, low wafer temperatures, and cells with high operating temperatures. For example, when the indium shutter is opened at an indium cell temperature of 980 °C, the apparent wafer temperature is increased by 26 °C, from 483 to 509 °C on a small wafer. For a larger wafer, opening the shutter of the Ga cell with the cell at 1095 °C induced apparent temperature increases from 463 to 487 °C (change of 24 °C) and from 581 to 584.5 °C (change of 3.5 °C). The spurious increases can be distinguished from actual heating of the wafer by the cell radiation based on the time scale of the changes. The most promising solution to this problem is to program the temperature measurements so they occur during brief growth interruptions when the shutters are closed. Correction factors for different growth conditions could also be used.

To put these results into perspective, the smart pyrometer improves the accuracy of temperature measurements in MBE by 10–20 °C over conventional pyrometry. The primary limitations are interference from light emitted by the effusion cells and noise-level signals at temperatures below 400 °C. The technique also depends on maintaining a specular sample surface and control over substrate wobble sufficient to allow absolute reflectance measurements to be made with an uncertainty of less than 2%. The extra effort to improve the accuracy of the temperature measurement is particularly of concern under growth conditions of heavy doping, very high or very low group V overpressure, or conditions where the sticking coefficient of a group III element or dopant is less than one. The changes in wafer temperature also occur slowly enough that the reflectance data acquired between temperature measurements is useful for determining layer thickness and composition.[14] The multifunctional nature of the optical system provides significant flexibility and increased ease of incorporation in the control structure of the growth system. The pyrometric technique could also be extended to other crystal-growth techniques such as organometallic vapor-phase epitaxy or to etching or deposition of nonmetallic films on silicon.

V. SUMMARY

A multifunctional optical system that measures both semiconductor wafer reflectance and emission has been shown to improve the accuracy of wafer temperature measurements by 10–20 °C. The system overcomes the primary limitation of conventional pyrometry under most MBE growth conditions by determining the sample emissivity each time a temperature measurement is made. We have shown that smart pyrometry is suitable for measuring temperatures from 400 °C and higher, with an uncertainty of 0.5 °C in the temperature range of 570 °C and above. The combined system can readily be calibrated with Al–Si eutectic wafers. For highest accuracy, temperature measurements must be taken with shutters closed on all high-temperature effusion cells.

ACKNOWLEDGMENTS

This work was supported in part by the Advanced Technology Program of the National Institute of Standards and Technology, U.S. Department of Commerce.

[1]E. Glazman, A. Glazman, and A. Thon, Mater. Res. Soc. Symp. Proc. **569**, 171 (1999).
[2]F. G. Böbel, H. Möller, A. Wowchak, B. Hertl, J. Van Hove, L. A. Chow, and P. P. Chow, J. Vac. Sci. Technol. B **12**, 1207 (1994).
[3]F. G. Böbel, H. Moeller, B. Hertel, G. Ritter, and P. Chow, Solid State Technol. August, 55 (1994).
[4]S. Johnson, C.-H. Kuo, M. Boonzaayer, W. Braun, U. Koelle, Y.-H. Zhang, and J. Roth, J. Vac. Sci. Technol. B **16**, 1502 (1998).
[5]E. S. Hellman and J. S. Harris, Jr., J. Cryst. Growth **81**, 38 (1987).
[6]F. Reif, *Fundamentals of Statistical and Thermal Physics* (McGraw–Hill, New York, 1965).
[7]A. A. Studna, D. E. Aspnes, L. T. Florez, B. J. Wilkens, J. P. Harbison, and R. E. Ryan, J. Vac. Sci. Technol. A 7, 3291 (1989).
[8]K. A. Bertness, R. K. Hickernell, and S. P. Hays, Mater. Res. Soc. Symp. Proc. **570**, 157 (1999).
[9]K. A. Bertness, R. K. Hickernell, S. P. Hays, and D. H. Christensen, J. Vac. Sci. Technol. B **16**, 1492 (1998).
[10]P. Thompson, Y. Li, J. J. Zhou, D. L. Sato, L. Fanders, and H. P. Lee, Appl. Phys. Lett. **70**, 1605 (1997).
[11]Y. M. Houng, M. R. T. Tan, B. W. Liang, S. Y. Wang, and D. E. Mars, J. Vac. Sci. Technol. B **12**, 1221 (1994).
[12]H. P. Lee, Y. Li, D. L. Sato, and J. J. Zhou, J. Vac. Sci. Technol. B **14**, 2151 (1996).
[13]R. N. Sacks, R. M. Sieg, and S. A. Ringel, J. Vac. Sci. Technol. B **14**, 2157 (1996).
[14]W. G. Breiland and K. P. Killeen, J. Appl. Phys. **78**, 6726 (1995).